ACS AGRICULTURAL SCIENCE & TECHNOLOGY

Open Access

pubs.acs.org/acsagscitech

Article

Nanosensors for Detecting Volatile Compounds in Pest Management: A Focus on Agricultural Sustainability

Published as part of ACS Agricultural Science & Technology special issue "Emerging Nano-Enabled Technologies for Sustainable Food and Agriculture".

Douglas A. Dias, Ilizandra A. Fernandes, Eliel P. Machado, Luiz Pedott, Maria Carolina Blassioli-Moraes, Miguel Borges, Juliana Steffens, and Clarice Steffens*

Cite This: https://doi.org/10.1021/acsagscitech.4c00531

Read Online

ACCESS | Metrics & More | Article Recommendations | Supporting Information

ABSTRACT: Traditional pest management strategies, such as indiscriminate pesticide use, have adverse environmental and human health implications. As a sustainable alternative, this research focuses on employing nanosensors for the detection of semiochemicals, including pheromones and defensive compounds, released by stink bugs. These nanosensors feature a nanohybrid layer of polyaniline and silver (PANI.Ag) and a nanocomposite of polyaniline and graphene oxide (PANI/GO). The study explores the detection of synthetic semiochemicals, including *cis* and *trans* bisabolene epoxides, (*E*)-2-hexanal, (*E*)-2-decenal, (*E*)-2-octenyl acetate, and (*E*)-2-octenal semiochemicals emitted by *Nezara viridula* (Southern green stink bug) in the real environment. The sensing layer characterization showed differences in hydrophilicity and surface roughness between the PANI.Ag and PANI/GO layers. When exposed to synthetic compounds like *cis* and *trans* bisabolene epoxides, (*E*)-2-hexanal, and (*E*)-2-decenal, the nanosensors demonstrated distinct responses, with PANI/GO exhibiting higher sensitivity. The resonance frequency shifts correlated with the concentration of the compounds, underscoring the potential of these sensors in detecting low concentrations with limits of detection (LOD) and quantification (LOQ) lower than 0.44 and 1.15 ng/mL, respectively. Real environment testing with soybean plants indicated that the nanosensors effectively detected semiochemicals emitted by *N. viridula* adults, especially in the presence of male−female couples, underscoring their potential for agricultural pest monitoring. The findings support the use of these nanosensors for the early detection of pest activity, offering a proactive approach to integrated pest management.

KEYWORDS: *nanosensors, pest management, stink bugs, semiochemicals*

INTRODUCTION

The agribusiness sector plays an increasingly pivotal role in global food production. Among various crops, soybeans have emerged as a significant agricultural activity due to their versatility and widespread cultivation, driven by the rising demand for human consumption, animal feedstock, and biofuel production.[1,2]

However, soybean cultivation is susceptible to attacks by various insect pests, notably stink bugs. Phytophagous stink bugs (order: Hemiptera) stand out as the most critical pests affecting soybeans (*Glycine max* (L.) Merrill) in Brazil.[3] Stink bug infestations can lead to plant development losses of up to 30%, causing misshapen and dried pods.[4]

Plants and insects communicate with their environment primarily through physical and chemical interactions. They possess highly sensitive and specific molecular recognition systems, without which they would not survive. These chemicals that facilitate communication between organisms are known as semiochemicals, and when they act within the same species, they are referred to as pheromones.[5]

The use of semiochemicals as a direct method for pest control or population monitoring presents a promising alternative to the indiscriminate use of pesticides, which can have adverse effects on the environment and human health. Male *Nezara viridula* L. stink bugs emit as sex pheromones two oxygenated sesquiterpenes: *cis* and *trans* epoxide-bisabolene.[6] Bioassays conducted in the laboratory with *N. viridula* from Brasilia, Brazil, have shown that females are specifically attracted to synthetic bisabolene epoxide.[7] Previous studies have identified that nymphs of *N. viridula* primarily produce unsaturated aldehydes such as (*E*)-2-hexenal, (*E*)-2-octenal, (*E*)-2-decenal, and 4-oxo-(*E*)-2-hexenal, along with linear hydrocarbons like undecane and tridecane.[8]

The development of new devices such as cantilever sensors for the detection of volatiles released by stink bug species is promising. Recent research demonstrates that nanosensors have become efficient in detecting stink bug pheromones (synthetic and in vivo), with high detection capacity and sensitivity.[9,10]

The aim of this research is to utilize nanocantilever sensors functionalized with a nanohybrid layer of polyaniline and silver

Received: September 2, 2024
Revised: September 27, 2024
Accepted: October 8, 2024

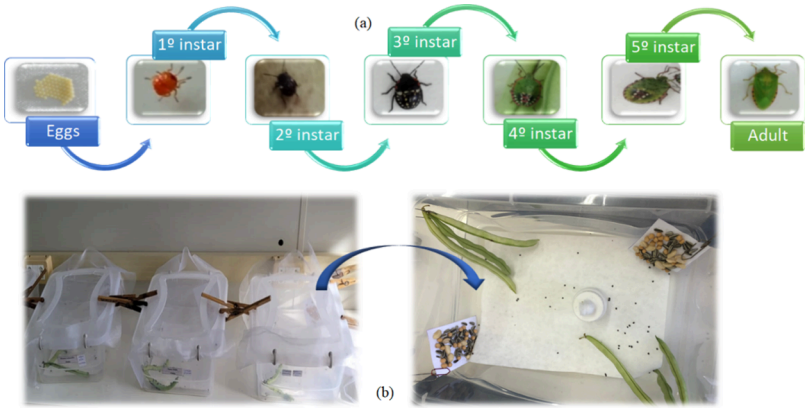

Figure 1. Stages of stink bug development and boxes with the insects.

(PANI.Ag) as well as polyaniline and graphene oxide (PANI/GO) for the detection of volatile compounds, including semiochemicals and defensive substances, produced and released by live *N. viridula* bugs. Additionally, these nanosensors will be applied to detect synthetic semiochemicals such as *cis* and *trans* bisabolene epoxides, (*E*)-2-hexanal, (*E*)-2-decenal, (*E*)-octenyl acetate, and (*E*)-2-octenal, as well as compounds emitted by stink bugs in their nymph and adult stages (males, females, and pairs). The study also includes real-environmental applications involving soybean plants.

MATERIALS AND METHODS

Functionalization of Cantilever Nanosensors. For this work, two cantilever nanosensors were developed: one with PANI.Ag and other with PANI/GO. A silicon cantilever (Budget Sensors) with a resonance frequency of 13 ± 4 kHz and a spring constant (k) of 0.2 N/m was used. A sensitive layer of PANI.Ag was obtained according to the methodology of Martinazzo et al.,[11] and the film was deposited on the cantilever surface by the dip coating technique. The layer of PANI/GO was developed following Brezolin et al.,[12] and the film was deposited by the layer-by-layer technique.

Characterization of the Nanosensor Surface. The chemical structures of PANI.Ag and PANI/GO nanocomposite films were characterized by atomic force microcopy (AFM, Nanosurf, Switzerland) with measurements in three different regions of the surface. To assess surface topography and roughness, an atomic force microscope (AFM, EasyScan 2 Flex, Switzerland) was employed in the tapping mode. The root-mean-square average (RMS) roughness was calculated at various positions within the image. Furthermore, the thickness of the immobilized layer on the cantilever was determined within a 50 μm^2 area.

Functional group analysis was performed using a PMI 550 spectrometer (KSV Instruments, Finland) through polarization modulation infrared reflection−absorption spectroscopy (PM-IRRAS). The spectrometer featured a spectral resolution of 8 cm^{-1}, and measurements were taken at an incident angle of 81°. A silicon-coated gold surface (1 × 1 cm), functionalized in a similar manner, served as the substrate.

Contact angle analysis was conducted both on uncoated cantilevers and after deposition of the sensing layer. This analysis was carried out using an apparatus from KSV Instruments, Finland, with ultrapure water droplets being used for the measurements.

The morphology of the sensing layers was analyzed by using scanning electron microscope (SEM). The SEM analysis was conducted at an operating voltage of 5 kV with a Zeiss EVO 28 instrument (Germany). Prior to imaging, the films were coated with a nanometric layer of platinum using a sputter coater (SCD 050—Balzers).

Synthetic Semiochemicals. The *cis* and *trans* bisabolene epoxides (1:1, v/v) were obtained from live insects as describe below; (*E*)-2-octenyl acetate was purchased from Bedoukian; and (*E*)-2-octenal, (*E*)-2-hexenal, and (*E*)-2-decenal were purchased from Sigma-Aldrich. These compounds were prepared in a range of concentrations (0.005, 0.01, 0.05, 0.1, 0.2, 0.3, 0.4, 0.5, 0.6, 0.7, 0.8, 0.9, and 1.0 μg/mL) by diluting them in hexane (99%, Vetec, Brazil), which served as the solvent. *cis* and *trans* Bisabolene epoxide were obtained from aeration samples of live males of *N. viridula* (for details, see Supporting Information).

Fourier Transform Infrared-Attenuated Total Reflectance (FTIR-ATR) Analysis. To evaluate the functional groups present in synthetic semiochemicals, attenuated total reflectance-Fourier transform infrared (ATR-FTIR) spectroscopy was employed. The infrared spectra were measured by using an Agilent spectrometer (Bruker Optic GmbH, Ettlingen, Germany) outfitted with a temperature-controlled single-bounce diamond ATR accessory. This setup also featured a deuterated triglycine sulfate (DTGS) detector. Each spectrum was recorded with 128 scans for both the sample and background, spanning the spectral range from 4000 to 800 cm^{-1} with a resolution of 2 cm^{-1}.

Nanosensor Response. A polypropylene sample injection chamber (gas sampling chamber) with a central upper opening (25 mm) and a height of 13 mm was used to accommodate the AFM scanner head (Nanosurf, C3000 Controller, Switzerland). The chamber contains two side openings for the entry and exit of volatile compounds as well as for cleaning purposes. Two rings with rubber seals were also used at the top to ensure complete protection during equipment fitting. The chamber was completely sealed to prevent the escape of gas molecules.

The nanosensor was inserted into the AFM cantilever holder, where the laser beam was adjusted to focus on the cantilever and its reflection was captured by the photodetector. The gas chamber was then attached to the cantilever holder and the contents were fully sealed. The resonance frequencies of the cantilever nanosensors were obtained by using a frequency analyzer. The measurements were configured in dynamic mode for the measurement procedure.

The experiments with synthetic volatile compounds at different concentrations involved first recording the resonance spectra of the cantilever nanosensors in synthetic air (control) for 90 s. Synthetic air was injected into the chamber through the one side opening, while the other side was left open. Next, 20 μL of each concentration of the sex pheromone was drawn with a syringe and injected into the gas sampling chamber by using a precise microsampler (Pipet-Lite XLS), where it was deposited onto a piece of filter paper (Milipore 25 μm) placed at the bottom of the chamber. After sampling, the system was purged with synthetic air prior to the next concentration.

Compounds Released by Live Insects. A mass rearing of stink bugs was conducted to obtain the insects to use as a pheromone source. Eggs of *N. viridula*, supplied by the Semiochemicals Laboratory at Embrapa Genetic Resources and Biotechnology in Brasília (DF), were used for this purpose. The eggs were placed in Petri dishes, which were sealed with a perforated plastic film to allow

https://doi.org/10.1021/acsagscitech.4c00531
ACS Agric. Sci. Technol. XXXX, XXX, XXX−XXX

Figure 2. Soybean plants (a) with annealed wire frames and nylon shade cloth (b), sealed containers with the plastic film (c), and injection of volatiles into the gas chamber (d).

air circulation. The insects remained in the dishes in a climate-controlled room at 25 °C until they reached the third instar. From the second instar onward, the stink bugs were fed green bean pods. Throughout their biological cycle, the stink bugs go through the stages of egg, nymph (comprising five instars), and adult, as shown in Figure 1.

After reaching the third instar, the insects were transferred to boxes (hermetic polyethylene boxes with a volume of 10 L). They were provided with a natural diet consisting of raw peanuts, soybeans, sunflower seeds, and green bean pods. The food was changed three times a week. To control humidity and provide water to the insects, disposable 100 mL containers with distilled water were used, maintaining the relative humidity of the air around 75%, monitored by a thermohygrometer (N322RHT, Novus, Brazil). The lids of the disposable containers had 1.0 cm diameter openings, through which a cotton wick was inserted to facilitate the water supply to the insects via capillary action. The boxes were sealed at the top with a mesh to allow air exchange with the environment. The stink bugs were kept under a photoperiod of 14 h of light (from 7 AM to 9 PM) and 10 h of darkness (from 9 PM to 7 AM).

For the pheromone release tests, nymphs (between the 4° and 5° instars), 10 males, 10 females, and 5 pairs were used. The insects were transferred from their rearing boxes to new boxes of the same size but without any food. Each box was sealed with a polyvinyl chloride film for 1 h to allow the concentration of volatiles. Subsequently, 20 μL of volatiles were collected using a gas syringe. The collected sample was then introduced into the chamber for measuring the resonance frequency of the cantilever nanosensors. Additionally, an identical box was evaluated under the same conditions but without the presence of insects. This box contained only insect food (beans, soybeans, peanuts, and sunflower seeds) and cotton soaked in water to assess any interference from volatiles released by these food sources.

Volatile collection from the nymphs was conducted daily, whereas for the adult insects, it was carried out every 2 days. The responses of both cantilever nanosensors (PANI.Ag and PANI/GO) were recorded using a frequency analyzer, following the same procedure as that for the synthetic compounds.

Real Environment Tests with Soybean Plants. To create a real environment, soybeans were cultivated using Pioneer 95R40 IPRO seeds, pretreated with LumiGEN (seed treatment). Sowing was done manually in December 2023, in 18 containers, with 2 seeds per container, using virgin forest soil with natural fertility from leaf litter. Each container was filled with approximately one-third of its volume in soil. From the time of sowing, the soil in each container was irrigated to meet the water requirements recommended for the crop. The first seedlings emerged 7 days after sowing.

Upon reaching the R_4 phenological stage, one plant was left per container. To introduce the insects into a real environment, the containers holding the soybean plants were transported to the laboratory, where structures of the annealed wire (1.80 m in length and 0.60 m in height per container) were assembled and covered with the 2.6 m^2 nylon shade cloth. The laboratory environment was maintained under controlled temperature and relative humidity conditions (N322RHT, Novus, Brazil) at 25 °C ± 1 and 57% ± 2 relative humidity.

For the semiochemical release tests, the containers were covered with polyethylene plastic bags (Figure 2). The detection of volatile compounds released by adult insects and soybean plants was conducted as follows: containers with only the soybean plant, a container with a soybean plant and 10 male stink bugs with around 10 days old on the adult phase, a container with a soybean plant and 10 female stink bugs, and a container with a soybean plant and pairs (5 males and 5 females). The insects were introduced into the containers and left to acclimate for 1 day before the experiments. One hour before the analysis, the containers were sealed with polyethylene plastic, and 20 μL of volatiles were collected with a gas microsyringe by piercing the plastic. The collected sample was immediately inserted into the gas chamber containing the nanosensors for resonance frequency measurement. The experiments were conducted over 5 days, with 2 analyses per day. All experiments were replicated for both plant analyses and nanosensor responses.

Characterization of Nanosensor Responses. The responses of the nanosensors to synthetic compounds were characterized in terms of linear sensitivity, limit of detection (LOD), and limit of quantification (LOQ). Linear sensitivity was determined from the slope of the calibration curve and the standard deviation of the analytical signal. The LOD, with a confidence level of 99.6%, was calculated as 3 times the standard deviation of the blank divided by the sensitivity. The LOQ was determined as 10 times the standard deviation of the blank divided by the sensitivity (n = 3).

Statistical Analysis. All analyses were performed in triplicate, and the results were subjected to analysis of variance (ANOVA) followed by T Student tests at a confidence level of 95% using Statistic 7.0 software.

RESULTS AND DISCUSSION

Sensor Layer Characterization. Figure 3 shows the PM-IRRAS spectra of PANI.Ag and PANI/GO layers deposited on the cantilever surface in the region between 990 and 1700 cm^{-1}. It is evident that the architectures were successfully functionalized, as indicated by the characteristic bands of

https://doi.org/10.1021/acsagscitech.4c00531
ACS Agric. Sci. Technol. XXXX, XXX, XXX−XXX

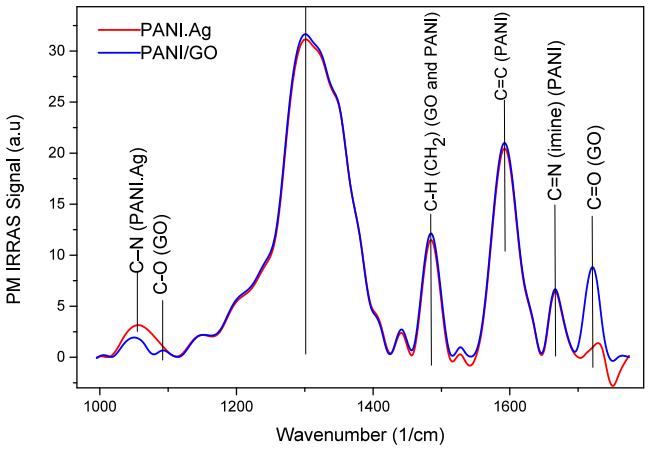

Figure 3. PM-IRRAS spectra of PANI.Ag and PANI/GO layers deposited on the cantilever surface.

PANI and GO (Table 1). The absence of significant changes in the dipole orientations following the functionalization with

Table 1. PM-IRRAS Wavenumbers of PANI.Ag and PANI/GO Layers Deposited on the Cantilever Surface

wavenumber (cm^{-1})	functional group
1087	C−O (graphene oxide)
1302	C−N (secondary aromatic amine) (PANI)
1484	C−H of CH_2 (PANI and GO)
1589	C=C (PANI)
1597−1620	C=N (imine) (PANI)
1722	C=O (GO)

silver (Ag) and GO is a noteworthy observation, signifying a high degree of molecular organization. This is reflected in the narrow peak widths observed in the PM-IRRAS spectra. Notable bands include the C−O band at 1087 cm^{-1}, corresponding to graphene oxide, and the C−N band at 1302 cm^{-1}, associated with secondary aromatic amines in PANI. The C−N stretching vibrations at 1057 cm^{-1} indicate that Ag interacted with the nitrogen atom of the PANI matrix.[13] The presence of the C−H band of CH_2 at 1484 cm^{-1} is indicative of both PANI and GO. The bands at 1589 cm^{-1} (C=C) and in the range 1597−1620 cm^{-1} (C=N imine) belong to PANI, attributed to the presence of quinoid and benzenoid rings in the emeraldine salt. The band at 1722 cm^{-1} corresponds to C=O in GO.[14]

Contact angle measurements indicate the wettability of a surface, where lower contact angles represent higher hydrophilicity (better wetting) and higher angles indicate greater hydrophobicity (poorer wetting). For PANI.Ag, a contact angle of 86.84° ± 0.32° was observed, suggesting a certain degree of hydrophilicity, reflecting its inherent surface characteristics. This phenomenon highlights the impact of Ag on improving surface properties and increasing the propensity for interactions with aqueous solutions. On the other hand, the PANI/GO film resulted in a higher contact angle (105.4° ± 0.4), suggesting a more hydrophobic surface. This observation aligns with the prevalence of the dispersive component of the surface energy, indicating a greater contribution from van der Waals forces. The increase in the contact angle and hydrophobicity of the PANI/GO film suggests interactions between GO and the PANI film, potentially leading to changes in the surface characteristics of the film. The increase in the contact angle is correlated with the highly hydrophobic nature of GO.

The results obtained in this study are consistent with the literature, emphasizing the adjustable surface properties of PANI-based materials when modified with Ag or GO. Taherian et al.[15] observed that graphene has a contact angle of 127° in water, characterizing it as a hydrophobic material with a smooth surface. The ability to control surface wettability through these modifications promises various applications, from sensors to coatings, where customized interactions with liquids are crucial. Ogihara et al.[16] also mentioned that low surface energy and high roughness result in a hydrophobic surface. Thus, the ability to adjust hydrophilicity or hydrophobicity through these modifications highlights the versatility and potential of PANI-based materials in different areas of application.

SEM and topographic images of the PANI.Ag and PANI/GO sensor layers revealed distinct characteristics regarding particle morphology and distribution (Figure 4). All samples exhibited a uniform structure well-adhered to the substrate surface. The surfaces showed variations in topography due to the presence of dispersed nanoparticles. PANI.Ag exhibited a uniform distribution of silver particles, while PANI/GO

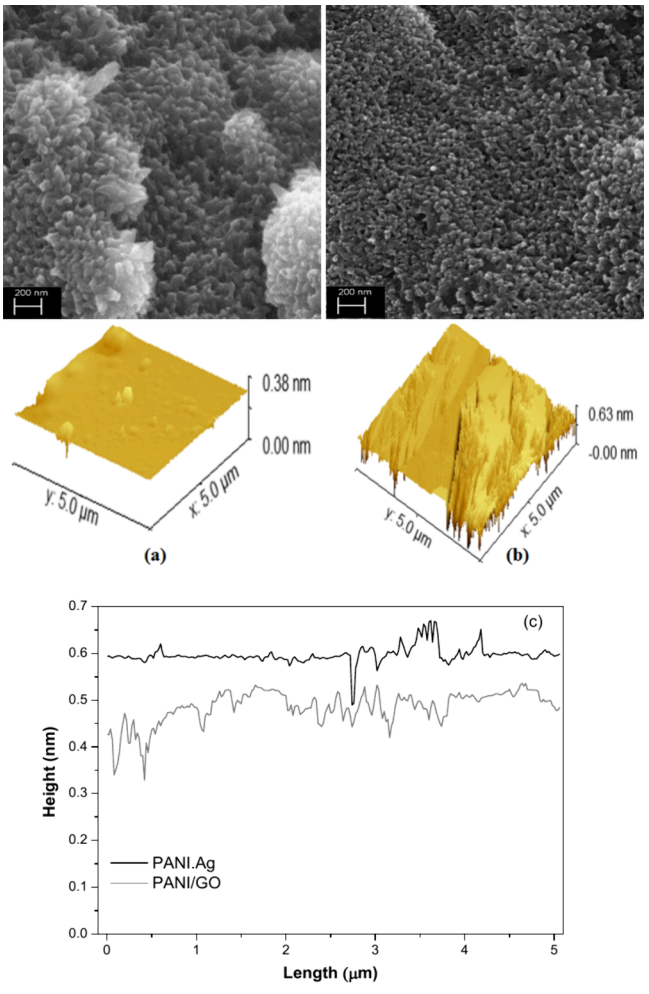

Figure 4. Morphological images (with a magnification of 5000×), topographic images, and height profile of PANI.Ag (a) and PANI/GO (b) sensor layers.

https://doi.org/10.1021/acsagscitech.4c00531
ACS Agric. Sci. Technol. XXXX, XXX, XXX−XXX

displayed a rougher topography due to the intertwined graphene sheets. The PANI.Ag surface showed lower roughness, corresponding to an average thickness of 0.45 nm, indicating a uniform distribution of silver particles over the PANI matrix. On the other hand, PANI/GO exhibited the highest roughness ($p < 0.05$), with an average thickness of 4.3 nm, highlighted by the presence of intertwined graphene oxide sheets that significantly contribute to this value (Table 2). The PANI.Ag surface is relatively smoother, which may limit the available surface area for adsorption. This could result in lower sensor sensitivity compared to PANI/GO, as there are fewer adsorption sites available for chemical interactions.

Table 2. Characterization of the Thickness and Roughness of the PANI.Ag and PANI/GO Layers[a]

layers	thickness (nm)	roughness (nm)
PANI.Ag	0.451[a] ± 0.126	9.350[b] ± 0.281
PANI/GO	0.430[a] ± 0.020	19.072[a] ± 7.114

[a]Mean (three repetitions) ± Standard Deviation. Equal letters in the column indicate no significant difference by the *T* Student test at 0.05 level.

Responses of Cantilever Nanosensors to Synthetic Compounds. The resonance frequency responses of the cantilever nanosensors with PANI.Ag and PANI/GO to volatile synthetic compounds such as *cis* and *trans* bisabolene epoxides, (*E*)-2-hexenal, (*E*)-2-decenal, (*E*)-2-octenyl acetate, (*E*)-2-octenal, synthetic air (control), and solvent hexane are presented in Figure 5.

Both the PANI.Ag and PANI/GO cantilever nanosensors exhibited a decrease in the resonance frequency with increasing concentrations of the synthetic compounds, indicating that the sensors responded to these substances. The detection mechanism of the cantilever nanosensor can be elucidated based on the chemical properties of these compounds. The

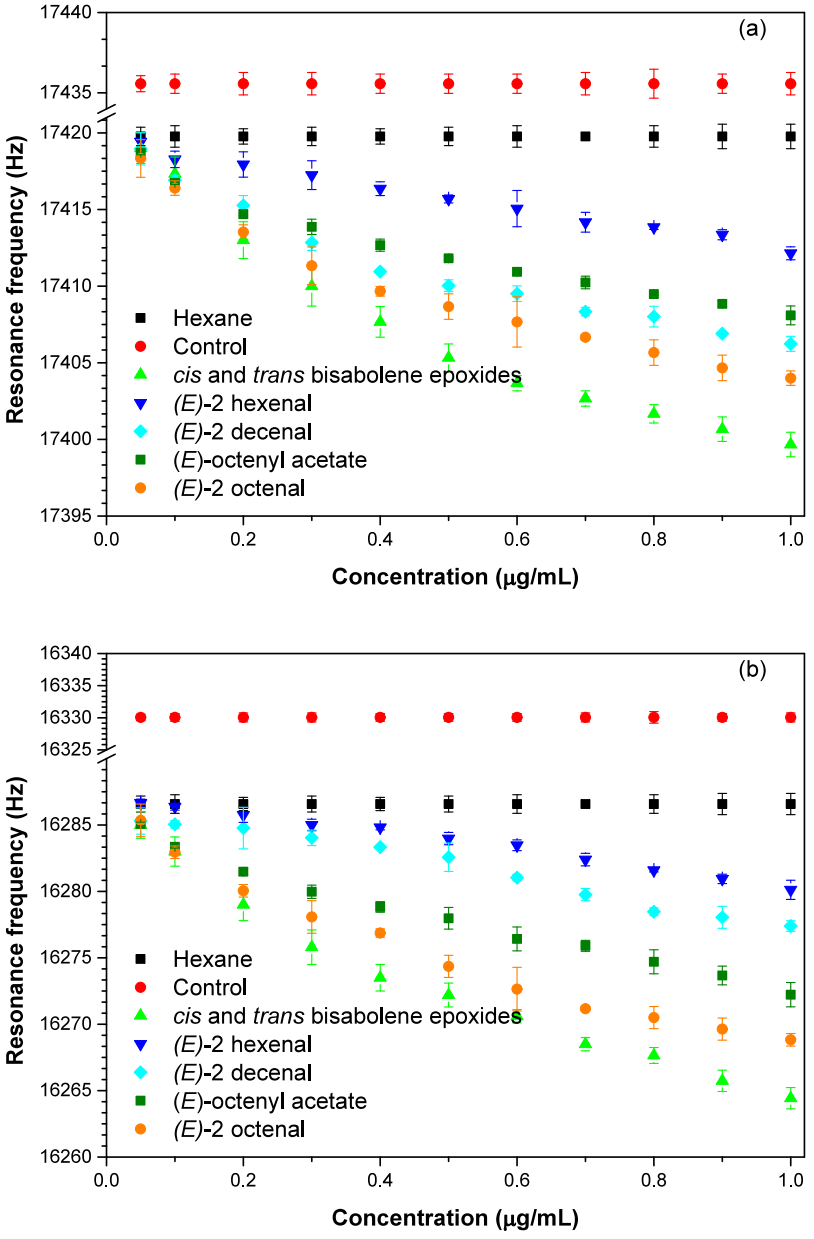

Figure 5. Resonance frequency response of PANI.Ag (a) and PANI/GO (b) cantilever nanosensors to the volatile compounds.

https://doi.org/10.1021/acsagscitech.4c00531
ACS Agric. Sci. Technol. XXXX, XXX, XXX−XXX

Table 3. Sensitivity, LOD, and LOQ of PANI.Ag and PANI/GO Cantilever Nanosensors for Synthetic Compounds *cis* and *trans* Bisabolene Epoxides, (*E*)-2-Hexenal, (*E*)-2-Decenal, (*E*)-2-Octenyl Acetate, and (*E*)-2-Octenal

	LOD (ng/mL^{-1})		LOQ (ng/mL)		sensitivity (Hz/ng·mL)		R^2	
synthetic compounds	PANI.Ag	PANI/GO	PANI.Ag	PANI/GO	PANI.Ag	PANI/GO	PANI.Ag	PANI/GO
cis and *trans* bisabolene epoxides	0.006	0.007	0.02	0.02	60.95	80.87	0.98	0.99
(*E*)-2- hexenal	0.04	0.44	0.10	1.15	10.85	7.02	0.98	0.97
(*E*)-2- decenal	0.08	0.14	0.31	0.52	6.56	8.45	0.98	0.97
(*E*)-2-octenyl acetate	0.35	0.26	1.12	0.93	4.97	14.27	0.97	0.97
(*E*)-2- octenal	0.28	0.20	0.95	0.78	6.19	8.15	0.99	0.98

presence of the epoxide group (C−O−C) imparts a certain degree of polarity to the molecules due to the electronegativity of oxygen. Additionally, both *trans*- and *cis*-(*Z*)-*α*-bisabolene epoxides have asymmetric carbons. Consequently, these bicyclic sesquiterpenes exhibit moderate to high vapor pressures due to their relatively low boiling points and weak intermolecular forces. The nanosensor, when coated with the composite (PANI with Ag or GO), can detect these isomers based on their specific chemical signatures, as they induce stress on the sensor upon contact due to molecular adsorption. This response was proportional to the concentration detected.

The amount of *cis* and *trans* bisabolene epoxides released by *N. viridula* can vary depending on the insect's life cycle. Generally, the release is higher during the reproductive period when the insect is seeking mating partners. Additionally, the quantity of pheromone released can also be influenced by environmental factors, such as temperature, humidity, and food availability.

In a study by Miklas et al.[17] using solid-phase microextraction (SPME) to investigate the sex pheromones emitted by *N. viridula* in various regions, significant differences were observed in the quantity of sex pheromones produced by males of the same species. However, notable consistency in the ratio of *cis* and *trans*-(*Z*)-bisabolene epoxides within each strain was also observed. This stability suggests a fundamental aspect of the species' chemical communication, possibly influenced by genetic or environmental factors.

Laboratory bioassays with *N. viridula* specimens from Brasília (DF) revealed that female insects showed attraction to synthetic *cis* and *trans*-(*Z*)-bisabolene epoxides when both isomers were present in the correct ratio.[7] This observation highlights the importance of the chemical composition and balance in eliciting behavioral responses in female *N. viridula*, providing insights into their complex mating behaviors and chemical communication mechanisms.

The compound (*E*)-2-decenal is a major aldehyde component of the metathoracic gland of adult *N. viridula*.[18] Additionally, (*E*)-2-decenal and (*Z*)-2-decenal are observed in first-instar nymphs. In second-instar nymphs, (*E*)-2-decenal, (*E*)-2-hexenal, and (*E*)-2-octenal appear.[19] The aggregation pheromone, which is mainly used by the nymphal stage stink bugs to attract others to suitable feeding or hibernation sites, consists of (*E*)-2-octenyl acetate, 4-oxo-(*E*)-2-hexenal, and (*E*)-2-hexenyl acetate. Both cantilever nanosensors responded to these compounds, especially at higher concentrations. The magnitude of the resonance frequency change is directly related to the amount of mass adsorbed on the cantilever surface. At higher concentrations of the compounds, more molecules are adsorbed on the surface, resulting in a more pronounced frequency change.

Table 3 presents the sensitivity, LOD, and LOQ results for PANI.Ag and PANI/GO nanosensors for synthetic compounds. The results indicate that both nanosensors can detect the analyzed compounds with LODs and LOQs in the ng/mL range, suitable for low-concentration detection applications. The nanosensor with PANI/GO generally demonstrated higher sensitivity to the compounds. When target molecules interact with the sensitive layer on the cantilever surface, they bind through various chemical forces, including hydrogen bonding, van der Waals forces, and electrostatic interactions, which induce structural changes. These changes, in turn, cause measurable shifts in the resonance frequency. Thus, the concentration of target molecules can be quantified with high sensitivity.

The FTIR-ATR analysis enabled the identification of characteristic absorption bands corresponding to various functional groups present in the synthetic compounds (Figure 6). Understanding their structures helps explain how these molecules interact with the sensing layers. The infrared spectra depicted distinct absorption patterns, notably intense absorptions at approximately 1640 cm^{-1} in the C=C stretching region for compounds like (*E*)-2-hexenal, (*E*)-2-octenyl acetate, and (*E*)-2-decenal. Additionally, absorptions around 1750 cm^{-1} were typical for carbonyl groups, observed in (*E*)-2-octenyl acetate and (*E*)-2-octenal, indicative of their aldehyde nature. All compounds exhibited characteristic C−H stretching

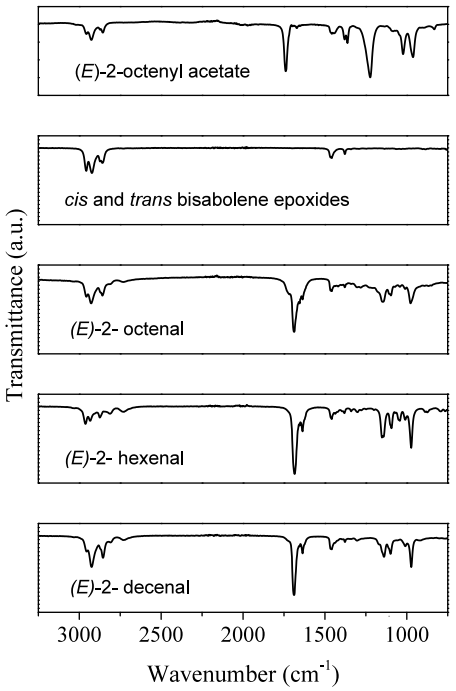

Figure 6. FTIR spectra of synthetic compounds showing characteristic functional groups.

https://doi.org/10.1021/acsagscitech.4c00531
ACS Agric. Sci. Technol. XXXX, XXX, XXX−XXX

vibrations from $-CH_2$ and $-CH_3$ groups (2850−3000 cm^{-1}), along with a band at 970 cm^{-1} corresponding to the bending vibration (C−H out of the plane). For *cis* and *trans* bisabolene epoxides, an absorption band at 2920 cm^{-1} corresponding to aliphatic CH vibrations was noted. Additionally, *cis* and *trans* bisabolene epoxides, (*E*)-2-hexenal, (*E*)-2-octenyl acetate, and (*E*)-2-decenal displayed a band at 1460 cm^{-1} attributed to the bending ($-CH_2$) of the alkyl chain and at 1360 cm^{-1} for the bending ($-CH_3$) of (*E*)-2-octenyl acetate. The stretching vibration of−C−O at 1130 cm^{-1} was observed for (*E*)-2-hexenal, (*E*)-2-octenyl acetate, (*E*)-2-decenal, and (*E*)-2-octenal, with an additional absorption at 1097 cm^{-1} for (*E*)-2-hexenal and (*E*)-2-decenal.

Based on specific functional groups detected by FTIR such as aldehydes (found in (*E*)-2-hexenal, (*E*)-2-decenal, and (*E*)-2-octenal) and esters (as in (*E*)-octenyl acetate) that directly influence the sensor response, aldehyde groups, characterized by prominent carbonyl stretches in the FTIR spectra, typically exhibit strong interactions with PANI-based sensors coated with PANI.Ag and PANI/GO. These interactions can lead to significant shifts in resonance frequency, reflecting the amount and affinity of the compound adsorbed. Similarly, aliphatic CH vibrations observed in compounds such as epoxy-bisabolene contribute to the overall interaction profile with the sensor surface, albeit to a lesser extent compared to carbonyl-containing compounds.

Responses to the Semiochemicals from In Vivo *N. viridula* in Boxes. The response of the cantilever nanosensors functionalized with PANI.Ag and PANI/GO to the volatile compounds from the blend of semiochemicals and defensive compounds released by *N. viridula* nymphs in the 4° and 5° instars, as well as adults and the control (synthetic air), is presented in Figure 7.

When exposed to synthetic air (control), the cantilever nanosensors did not show any variation in the resonance frequency (Hz). The 4° and 5° instar phases lasted on average 15 days. During the nymph stages, a slight change in resonance frequency (2 Hz) was observed, while in the adult stage, an increase was noted for both sensors. This indicates that adults release semiochemicals in larger quantities, which may be related to the higher body mass of the adults compared to nymphs and with the higher level of activities involved in the adult life such as mating behavior, foraging, or territorial defense. The increased metabolic activity and production of semiochemicals during the adult phase likely result in greater exposure and, consequently, a more pronounced nanosensor response. The observed variations during these phases are attributed to fluctuations in the amount of volatile compounds collected in the boxes.

Response of Sensors to Semiochemicals in a Real Environment. The resonance frequency responses to synthetic air (control) showed no variation over time, indicating the stability of the nanosensors in this environment without detectable external influences (Figure 8). When volatiles emitted solely by soybean plants were evaluated, no significant change in resonance frequency was observed, suggesting that these volatiles did not measurably affect the sensor response during the evaluation period. Plants when are not under injury release very tiny quantity of volatiles.[20,21] Stink bugs are sucking insects; therefore, they provoke very tiny injuries in plants, and several studies have shown that plants take time to respond to injury of sucking insects,[21−23] it is necessary at least 48 h or more to plants start to activate

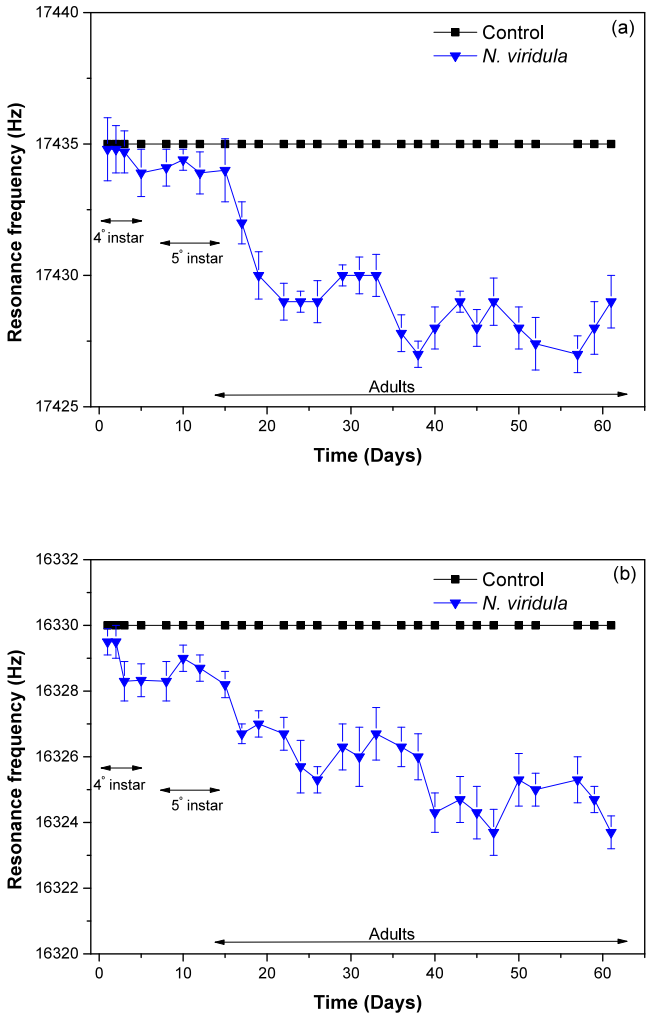

Figure 7. Response of the cantilever nanosensors with PANI.Ag (a) and PANI/GO (b) exposed to the in vivo compounds from *N. viridula* nymphs in the 4° and 5° instars and in the adult stage.

their defense response and start to release volatiles. In our study the insects were allowed to feed on plants for 24 h, and the plants were not releasing the herbivore-induced plant volatiles. Further studies could evaluate the nanosensors' response at different time points to better address this issue.

However, upon introduction of the insects, variations in the resonance frequency of the nanosensors were observed. These variations were more pronounced in environments containing couples and males of stink bugs. The most significant variation was specifically noted in the environment with couples, which was attributed to the release of sex pheromones by males to attract females for mating. The absence of response in females, as observed in the experiments, suggests that females were not releasing defensive compounds from metathoracic glands, which indicates that the insects were in an adequate environment. The insects when are safe do not release defensive compounds from metathoracic glands, and in general, males release only the sex pheromone.[24] This indicates that probably the males were releasing the sex pheromones, and what was detected in the PANI.Ag and PANI/GO nanosensors was the sex pheromones produced by males.

The sexual pheromones released by males are detected by the highly sensitive antennae of females, which are equipped with specialized receptors capable of recognizing and

https://doi.org/10.1021/acsagscitech.4c00531
ACS Agric. Sci. Technol. XXXX, XXX, XXX−XXX

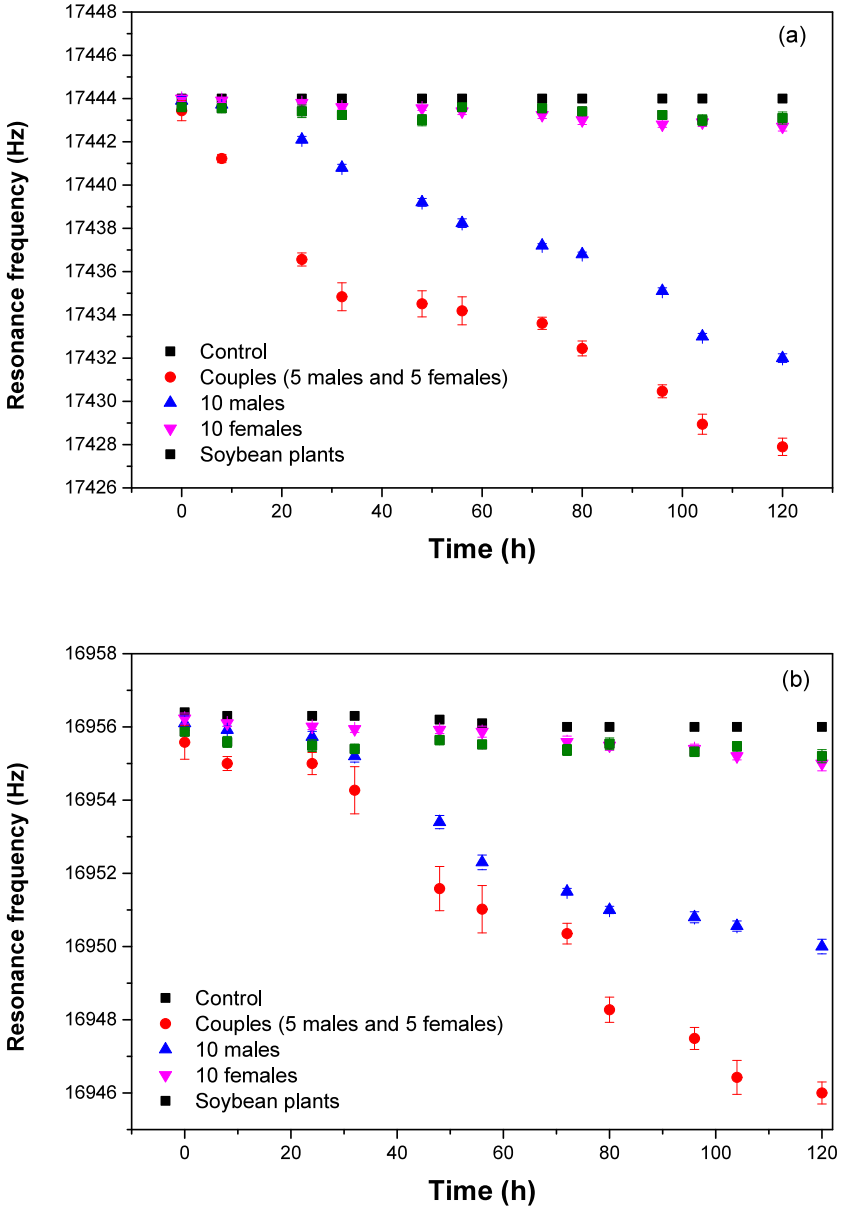

Figure 8. Response of PANI.Ag (a) and PANI/GO (b) cantilever nanosensors exposed to in vivo compounds of *N. viridula* in a real environment.

responding to specific chemical signals. This allows females to locate males and respond to mating signals.[25]

Thus, detecting these compounds in a real environment containing soybean plants with nanosensors indicates the presence and activity of the stink bugs, as these compounds are specific to sexual communication and are primarily released by males to attract females. The ability to detect these chemical signals is important for monitoring the presence and behavior of these insects in soybean fields and other agricultural settings.

The study of these compounds has validated the fundamental biological mechanisms involved in intraspecific communication among stink bugs and has significant practical applications in integrated pest management and agricultural crop conservation. By gaining a deeper understanding of how stink bugs utilize pheromones for mating, farmers can devise more effective monitoring and control strategies, thus, reducing pesticide use and minimizing environmental impacts. Additionally, nanosensors can be deployed in agricultural fields to detect the presence of pheromones well before large-scale pest infestations occur. This proactive approach helps farmers schedule targeted pest control measures more effectively.

For future research, it is crucial to investigate the pheromone release rates of insects, measured per hour and per acre, as these data are currently lacking in the literature for *N. viridula*. Subsequent studies should focus on analyzing this release and detection using nanosensors, which could provide valuable insights into the dynamics of pheromone emissions and enhance the effectiveness of pest management strategies.

CONCLUSIONS

The study successfully demonstrated the potential of cantilever nanosensors functionalized with PANI.Ag and PANI/GO for detecting volatile organic compounds and semiochemicals emitted by *N. viridula*. The characterization of the sensors using PM-IRRAS and SEM confirmed effective functionalization and provided insights into the molecular interactions on the sensor surface. The sensors exhibited distinct responses to various synthetic compounds, with PANI/GO showing higher

https://doi.org/10.1021/acsagscitech.4c00531
ACS Agric. Sci. Technol. XXXX, XXX, XXX−XXX

sensitivity, particularly to aldehydes and esters, which are prominent in stink bug emissions.

In real-environment tests conducted with soybean plants, the sensors effectively detected semioil chemicals released by *N. viridula* under natural conditions. Both nanosensors demonstrated sensitivity to the semiochemicals present in the emissions from the insects on soybean plants, validating its potential application in agricultural settings. These findings suggest that PANI-based nanosensors could be a valuable tool for early pest detection in agriculture, enabling timely and targeted interventions.

■ ASSOCIATED CONTENT

Data Availability Statement

Data will be made available on request.

Supporting Information

The Supporting Information is available free of charge at https://pubs.acs.org/doi/10.1021/acsagscitech.4c00531.

Methodology for collecting volatiles from male *N. viridula*, detailing the setup of the glass containers, air flow specifications, feeding regimen, and trap elution processes; the purification procedure for *cis* and *trans* bisabolene epoxide through liquid chromatography, specifying the column parameters, elution solvents, and concentration techniques used; and analytical techniques, including gas chromatography (GC) and gas chromatography−mass spectrometry (GC−MS) parameters, instrumentation, and temperature programs (PDF)

■ AUTHOR INFORMATION

Corresponding Author

Clarice Steffens − *Food Engineering, URI—Erechim, Erechim, Rio Grande do Sul 99709-910, Brazil;* orcid.org/0000-0003-4394-125X; Email: clarices@uricer.edu.br

Authors

Douglas A. Dias − *Food Engineering, URI—Erechim, Erechim, Rio Grande do Sul 99709-910, Brazil*

Ilizandra A. Fernandes − *Food Engineering, URI—Erechim, Erechim, Rio Grande do Sul 99709-910, Brazil*

Eliel P. Machado − *Food Engineering, URI—Erechim, Erechim, Rio Grande do Sul 99709-910, Brazil*

Luiz Pedott − *Food Engineering, URI—Erechim, Erechim, Rio Grande do Sul 99709-910, Brazil*

Maria Carolina Blassioli-Moraes − *Embrapa Genetic Resources and Biotechnology, Brasília, Distrito Federal 70770-917, Brazil*

Miguel Borges − *Embrapa Genetic Resources and Biotechnology, Brasília, Distrito Federal 70770-917, Brazil*

Juliana Steffens − *Food Engineering, URI—Erechim, Erechim, Rio Grande do Sul 99709-910, Brazil*

Complete contact information is available at: https://pubs.acs.org/10.1021/acsagscitech.4c00531

Funding

The Article Processing Charge for the publication of this research was funded by the Coordination for the Improvement of Higher Education Personnel - CAPES (ROR identifier: 00x0ma614).

Notes

The authors declare no competing financial interest.

■ ACKNOWLEDGMENTS

This work was supported by the National Council for Scientific and Technological Development—Brazil (CNPq), Coordination for the Improvement of Higher Education Personnel—Brazil (CAPES)—Finance Code 001, and Research Support Foundation of the State of Rio Grande of Sul—Brazil (FAPERGS), and we thank Financiadora de Estudos e Projetos (FINEP) for their financial support. This study also was supported in part by the INCT Nanotechnology for Sustainable Agriculture (National Council for Scientific and Technological Development (CNPq) #405924/2022-4; Coordenação de Aperfeiçoamento de Pessoal de Nível Superior—Brasil (CAPES), São Paulo Research Foundation (FAPESP), and Fundação de Pesquisa do Distrito Fderal—FAPD_ No. 00193.00001056/2021-68.

■ REFERENCES

(1) Song, X.-P.; Hansen, M. C.; Potapov, P.; Adusei, B.; Pickering, J.; Adami, M.; Lima, A.; Zalles, V.; Stehman, S. V.; Di Bella, C. M.; Conde, M. C.; Copati, E. J.; Fernandes, L. B.; Hernandez-Serna, A.; Jantz, S. M.; Pickens, A. H.; Turubanova, S.; Tyukavina, A. Massive Soybean Expansion in South America since 2000 and Implications for Conservation. *Nat. Sustain.* **2021**, *4* (9), 784−792.

(2) da Silva, R. F. B.; Viña, A.; Moran, E. F.; Dou, Y.; Batistella, M.; Liu, J. Socioeconomic and Environmental Effects of Soybean Production in Metacoupled Systems. *Sci. Rep.* **2021**, *11* (1), 18662.

(3) Fernandes, P. H. R.; Ávila, C. J.; da Silva, I. F.; Zulin, D. Damage by the Green-Belly Stink Bug to Corn. *Pesqui. Agropecuária Bras.* **2020**, *55*, No. e01131.

(4) Hayashida, R.; Hoback, W. W.; de Freitas Bueno, A. A Test of Economic Thresholds for Soybeans Exposed to Stink Bugs and Defoliation. *Crop Prot.* **2023**, *164*, No. 106128.

(5) Čokl, A.; Žunič-Kosi, A.; Stritih-Peljhan, N.; Blassioli-Moraes, M. C.; Laumann, R. A.; Borges, M. Stink Bug Communication and Signal Detection in a Plant Environment. *Insects* **2021**, *12* (12), 1058−1081.

(6) Baker, R.; Borges, M.; Cooke, N. G.; Herbert, R. H. Identification and Synthesis of (Z)-(1′S,3′R,4′S)(−)-2-(3′,4′-Epoxy-4′-Methylcyclohexyl)-6-Methylhepta-2,5-Diene, the Sex Pheromone of the Southern Green Stinkbug, Nezara Viridula(L.). *J. Chem. Soc. Chem. Commun.* **1987**, *6*, 414−416.

(7) Borges, M. Attractant Compounds of the Southern Green Stink Bug, Nezara Viridula (L.) (Heteroptera: Pentatomidae). *An. da Soc. Entomológica do Bras* **1995**, *24* (2), 215−225.

(8) Moraes, M. C. B.; Pareja, M.; Laumann, R. A.; Borges, M. The Chemical Volatiles (Semiochemicals) Produced by Neotropical Stink Bugs (Hemiptera: Pentatomidae). *Neotrop. Entomol.* **2008**, *37* (5), 489−505.

(9) Martinazzo, J.; Brezolin, A. N.; Paschoalin, R. T.; Soares, A. C.; Steffens, J.; Steffens, C. Sexual Pheromone Detection Using PANI·Ag Nanohybrid and PANI/PSS Nanocomposite Nanosensors. *Anal. Methods* **2021**, *13* (35), 3900−3908.

(10) Brezolin, A. N.; Martinazzo, J.; Steffens, J.; Steffens, C. Nanostructured Cantilever Sensor Using with Pani/MWCNT-COOH Nanocomposites Applied in the Detection of Pheromone. *J. Mater. Sci. Mater. Electron.* **2020**, *31*, 6008−6016.

(11) Martinazzo, J.; Ballen, S. C.; Steffens, J.; Steffens, C. Sensing of Pheromones from *Euschistus heros* (F.) Stink Bugs by Nanosensors. *Sensors and Actuators Reports* **2022**, *4*, No. 100071.

(12) Brezolin, A. N.; Martinazzo, J.; Steffens, J.; Steffens, C. Polyaniline−Graphene Oxide Nanocomposite Microelectromechanical Sensor for Stink Bugs Pheromone Detection. *Sensors Actuators B Chem.* **2020**, *305*, No. 127426.

(13) Badry, R.; Shaban, H.; Elhaes, H.; Refaat, A.; Ibrahim, M. Molecular Modeling Analyses of Polyaniline Substituted with Alkali and Alkaline Earth Elements. *Biointerface Res. Appl. Chem.* **2018**, *8* (6), 3719−3724.

(14) Mutalib, T. N. A. B. T. A.; Tan, S. J.; Foo, K. L.; Liew, Y. M.; Heah, C. Y.; Abdullah, M. M. A. B. Properties of Polyaniline/Graphene Oxide (PANI/GO) Composites: Effect of GO Loading. *Polym. Bull.* **2021**, *78* (9), 4835−4847.
(15) Taherian, F.; Marcon, V.; van der Vegt, N. F. A.; Leroy, F. What Is the Contact Angle of Water on Graphene? *Langmuir* **2013**, *29* (5), 1457−1465.
(16) Ogihara, H.; Xie, J.; Okagaki, J.; Saji, T. Simple Method for Preparing Superhydrophobic Paper: Spray-Deposited Hydrophobic Silica Nanoparticle Coatings Exhibit High Water-Repellency and Transparency. *Langmuir* **2012**, *28* (10), 4605−4608.
(17) Miklas, N.; Renou, M.; Malosse, I.; Malosse, C. Repeatability of Pheromone Blend Composition in Individual Males of the Southern Green Stink Bug. *Nezara viridula. J. Chem. Ecol.* **2000**, *26* (11), 2473−2485.
(18) Aldrich, J. R.; Oliver, J. E.; Lusby, W. R.; Kochansky, J. P.; Lockwood, J. A. Pheromone Strains of the Cosmopolitan Pest, *Nezara viridula* (Heteroptera: Pentatomidae). *J. Exp. Zool.* **1987**, *244* (1), 171−175.
(19) Fucarino, A.; Millar, J. G.; McElfresh, J. S.; Colazza, S. Chemical and Physical Signals Mediating Conspecific and Heterospecific Aggregation Behavior of First Instar Stink Bugs. *J. Chem. Ecol.* **2004**, *30* (6), 1257−1269.
(20) Carolina Blassioli Moraes, M.; Laumann, R.; Sujii, E. R.; Pires, C.; Borges, M. Induced Volatiles in Soybean and Pigeon Pea Plants Artificially Infested with the Neotropical Brown Stink Bug, *Euschistus heros*, and Their Effect on the Egg Parasitoid, Telenomus Podisi. *Entomol. Exp. Appl.* **2005**, *115* (1), 227−237.
(21) Michereff, M. F. F.; Laumann, R. A.; Borges, M.; Michereff-Filho, M.; Diniz, I. R.; Farias Neto, A. L.; Moraes, M. C. B. Volatiles Mediating a Plant-Herbivore-Natural Enemy Interaction in Resistant and Susceptible Soybean Cultivars. *J. Chem. Ecol.* **2011**, *37* (3), 273−285.
(22) Nascimento, I. N.; Michereff, M. F. F.; Pereira, W. E.; Villas-Boas, P. R.; Gusmão, M. R.; Caufield, J.; Laumann, R. A.; Borges, M.; Blassioli-Moraes, M. C. Role of Herbivore-Induced Maize Volatiles in the Chemotactic Behaviour of *Telenomus podisi* and *Diceraeus melacanthus*. *Entomol. Exp. Appl.* **2023**, *171* (3), 196−205.
(23) Colazza, S.; McElfresh, J. S.; Millar, J. G. Identification of Volatile Synomones, Induced by *Nezara viridula* Feeding and Oviposition on Bean Spp., That Attract the Egg Parasitoid Trissolcus Basalis. *J. Chem. Ecol* **2004**, *30* (5), 945−964.
(24) Borges, M.; Blassioli-Moraes, M. C. Chapter 5 The Semiochemistry of Pentatomidae. In *Stink Bugs*; Čokl, A.; Borges, M., Eds.; CRC Press, 2017; pp 95−124.
(25) Brezolin, A. N.; Martinazzo, J.; Muenchen, D. K.; de Cezaro, A. M.; Rigo, A. A.; Steffens, C.; Steffens, J.; Blassioli-Moraes, M. C.; Borges, M. Tools for Detecting Insect Semiochemicals: A Review. *Anal. Bioanal. Chem.* **2018**, *410* (17), 4091−4108.

https://doi.org/10.1021/acsagscitech.4c00531
ACS Agric. Sci. Technol. XXXX, XXX, XXX−XXX